

# A study on the Diffusion Charge Redistribution strategy in Photovoltaics optimization

Ana C. A. Barbosa  
Department of informatics  
State University of Ponta Grossa  
Ponta Grossa, Brazil  
anacbse@gmail.com

André A. Mariano  
Department of Electrical Engineering  
Federal University of Paraná  
Curitiba, Brazil  
mariano@eletrica.ufpr.br

Juan C. Castellanos  
Department of informatics  
State University of Ponta Grossa  
Ponta Grossa, Brazil  
jccastellanosro@gmail.com

**Abstract**—Maximum power point tracking (MPPT) has been a recurring topic research in photovoltaics (PV) optimization as it can maximize the amount of power produced by these technologies. However, these methods can not rise their maximum power point (MPP) level as it drops under nonuniform irradiance by different causes. The diffusion charge redistribution (DCR) strategy raises the MPP of mismatched PV systems while not affecting their convex characteristics curves. This simplifies MPPT methods such as artificial neural networks (ANNs) used to predict an MPP related output. Here, the DCR strategy is explored in an on-chip system using a ladder structure together with an ANN for MPPT to elevate the power processed by PVs.

**Index Terms**—diffusion charge redistribution, photovoltaics optimization, maximum power point tracking, artificial neural networks

## I. INTRODUCTION

As the presence of photovoltaic (PV) grows stronger due to its clean and renewable energy source, maximum power point tracking (MPPT) methods becomes a relevant research topic in PVs optimization as shown in [1]–[3]. However, the development of techniques that can raise the maximum power point (MPP) of PVs is also necessary to still extract a great amount of energy under mismatch conditions.

Mismatch drops the MPP level of PVs in a series circuit (designated string) to a minimum as their output current is limited by their weakest component. Because it occurs when the installations are under nonuniform irradiance [4], it becomes a big problem where shading is unpredictable, mostly in urban areas and in dry regions where the accumulation of dust tends to be inevitable [5]. This can jeopardize the performance of applications that use solar harvesting such as wireless sensor networks (WSNs).

A common way of counter mismatch in PV modules has been the use of bypass diodes. They are associated in parallel with the cells and so create an additional path for the module's current. This method raises the MPP level with the trade-off of creating nonconvex characteristic curves [6], [7] thus troubling MPPT methods as there are local maximas.

The recent diffusion charge redistribution (DCR) strategy [8] shows that it can appreciably raise the MPP level of mismatched PVs while maintaining their default convex characteristics. It can be easily integrated on-chip which makes it a powerful method for recent applications, e.g. internet of

things (IoT), where integrated renewable power solutions are becoming desirable [9].

In this paper, we explore the DCR strategy together with an artificial neural network (ANN) based MPP prediction method. ANNs have been used to predict an MPP related output given the PV's characteristics or parameters [10]. Once this prediction is done, the system can be induced to operate in its MPP by hardware means. As DCR does not affect the convex characteristics of PVs, the use of an ANN for MPPT demands low level of complexity. Therefore, its implementation does not jeopardize the power efficiency and area of the solution on-chip.

Section II presents the modelling of the PV cell used in this study. Section III discusses a ladder DCR structure and presents its behaviour in Cadence simulation environment. Section IV shows the ANN that can be used to find the MPP of the proposed DCR structure. Section V concludes this work and proposes possible future ones in this matter.

## II. PV CELL MODEL

The five-parameter single diode PV cell modelling as proposed in [11] is used in this work. It characterizes the PV cell by its photovoltaic current  $I_L$ , its diode's saturation current  $I_D$ , its internal ohmic resistances  $R_{sh}$  and  $R_s$  and the diode's ideality factor  $N$ . Using the experimental data of the PV cell presented in [8], the five-model parameters were extracted as shown in Table I. They belong to a monocrystalline P-Maxx-2500 mA solar cell with 1.5 A short circuit current ( $I_{SC}$ ), a 0.52 V open circuit voltage ( $V_{OC}$ ), a 1.25 A MPP current ( $I_{mp}$ ) and a 0.42 V MPP voltage ( $V_{mp}$ ).

To apply DCR, the diffusion capacitance  $C_d$  is included in the PV cell model. This additional parameter, modelled in Verilog language, shows a dependency on the cell's  $I_D$  [8] and its value is given by (1) as follows:

$$C_d = 4.64\mu F + 9.06 \left( \frac{\mu F}{A} \right) \cdot I_D \quad (1)$$

The final PV cell model is shown in Fig. 1.

## III. LADDER DCR STRUCTURE

The DCR strategy optimizes the efficiency of PV circuits by redistributing charge between its components through their

TABLE I  
PV CELL PARAMETERS

Parameter	Value	Unit
$I_L$	1.526	A
$I_D$	22.143	fA
$R_{sh}$	2.257	$\Omega$
$R_s$	0.039	$\Omega$
$N$	0.630	-

own cell's diffusion capacitances. Fig. 2 shows a  $m : n$  ladder PV string,  $m$  and  $n$  being the number of cells with odd and even assigned designators, respectively, able to change its structure by switching phases  $\varphi_1$  and  $\varphi_2$ . This makes the cells appear in pseudo-parallel and mitigates string's mismatch losses. The technique does not require external storage components and eases its implementation in an integrated circuit.

The proposed switching process inserts losses in the DCR strategy, as shown in [8]'s switched capacitor conversion loss analysis adapted from [12]:

$$IL_{SSL} = \frac{1}{12} \cdot \frac{m-1}{m} \cdot \frac{1}{f_{sw}} \cdot \frac{1}{V_{mp}} \cdot \frac{I_{mp}}{C_d} \quad (2)$$

$$IL_{FSL} = \frac{4}{2m-1} \cdot \frac{m-1}{m} \cdot \frac{I_{mp}}{V_{mp}} \cdot R_{eff} \quad (3)$$

$$IL_{TOTAL} \cong \sqrt{(IL_{SSL})^2 + (IL_{FSL})^2} \quad (4)$$

where  $f_{sw}$  is the switching frequency,  $R_{eff}$  is the switch's effective on-resistance,  $IL_{SSL}$  and  $IL_{FSL}$  are the slow-switching and fast-switching limit losses related, respectively, and  $IL_{TOTAL}$  is the total loss of the switching process. This shows that the total loss of the structure used in this work is a small amount of 0.12% considering maximum uniform illumination and a  $R_{eff}$  of 1m $\Omega$ .

The 3 : 2 ladder DCR string was simulated in Cadence Virtuoso Analog Design Environment with a duty cycle of 50% and a switching frequency of 50 kHz. Fig. 3 shows the schematic of the circuit used in the simulations. A transient simulation of 100  $\mu$ s was performed and the system output voltage ( $V_{OUT}$ ) and load current ( $I_{load}$ ) were measured so only the steady-state of the aforementioned signals would be used to compute the results shown next (which means after 60 ns, as shown in Fig. 4).

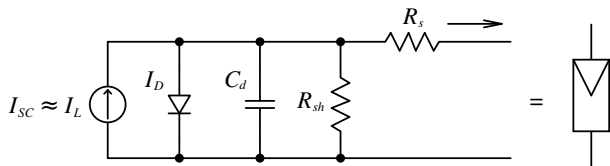


Fig. 1. PV cell model.

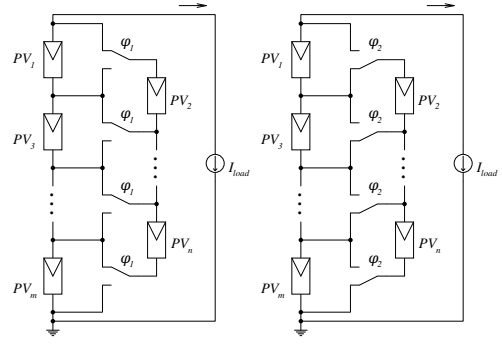


Fig. 2. A PV  $m : n$  ladder string using DCR strategy.

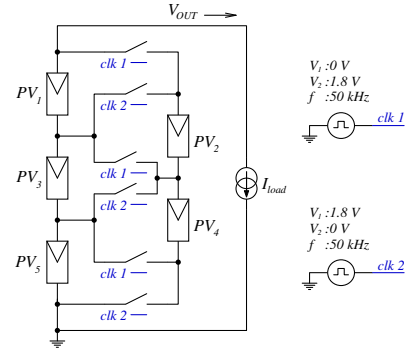


Fig. 3. Schematic of the 3 : 2 ladder DCR string used for simulation in Cadence environment:  $clk 1$  and  $clk 2$  are the switches' control signals.

The evident advantage of DCR can be seen in the simulations results shown in Fig. 5, where the performance of a PV 5-cell string, its commercial approach using bypass diodes and the 3 : 2 ladder DCR string are compared. The DCR provides near 60% more output power than its commercial counterpart. Fig. 5 also confirms that the characteristics of the DCR structure are still convex under mismatch, reinforced by the different shading conditions applied to this configuration (Fig. 6). Fig. 7 shows the maximum output power ( $P_{mp}$ ) of the bypassed 5-cell and the 3 : 2 ladder DCR strings under different shading conditions for the clarification of the DCR strategy optimization.

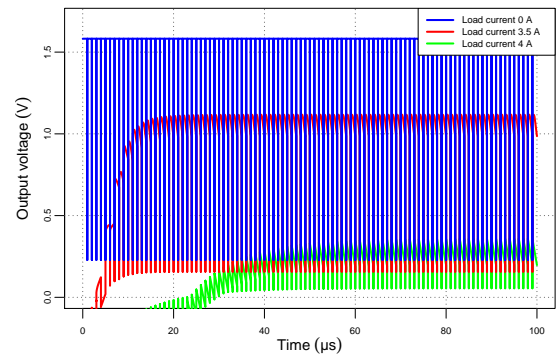


Fig. 4. Transient voltage for different values of load current. The signal is steady-state after 60  $\mu$ s.

#### IV. ANN BASED MPP PREDICTION METHOD

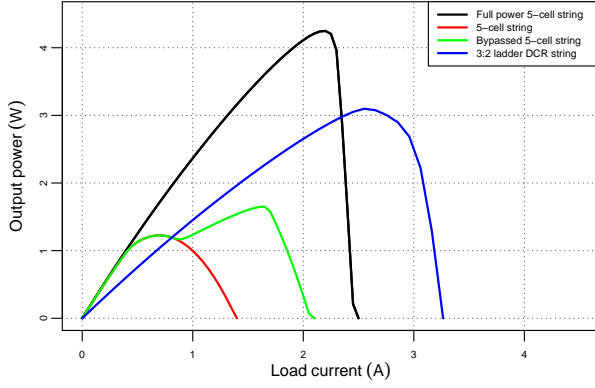


Fig. 5. Simulation results of the 5-cell string (red solid line), the diode bypassed 5-cell string (green solid line) and the 3 : 2 ladder DCR string (blue solid line) under same shading condition (2 shaded cells; 1 cell 25% shaded, 1 cell 75% shaded). The 5-cell string without shading condition (black solid line) is plotted for power loss comparison.

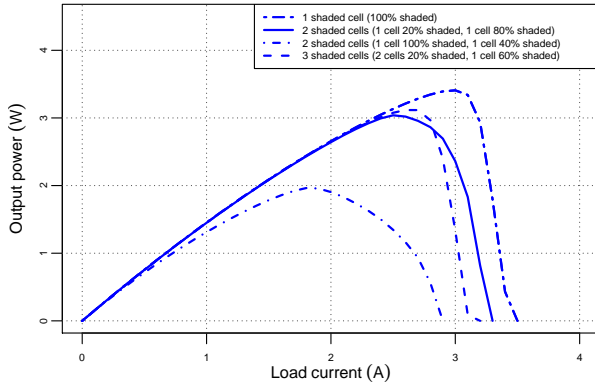


Fig. 6. Simulation results of the 3 : 2 ladder DCR string under different shading conditions: 1 cell 100% shaded (two-dashed line), 1 cell 20% shaded and 1 cell 80% shaded (solid line), 1 cell 100% shaded and 1 cell 40% shaded (dot-dashed line) and 2 cells 20% shaded and 1 cell 60% shaded (dashed line).

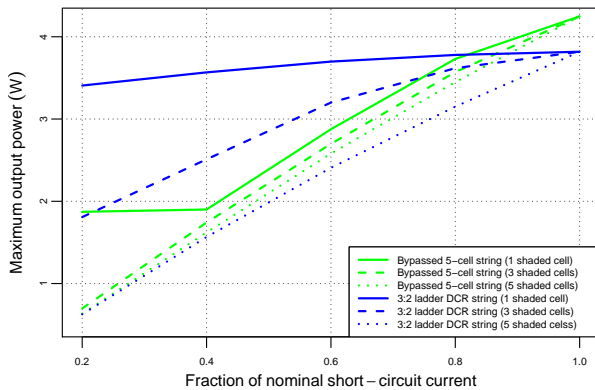


Fig. 7. Simulation results of the bypassed 5-cell string (green line) and the 3 : 2 ladder DCR string (blue line) under different shading conditions: 1 shaded cell (solid line), 3 shaded cells (dashed line) and 5 shaded cells (dotted line).

ANNs are commonly applied to regression problems for their ability in predicting outputs given their inputs [13]. They can be represented as a three layer weighted directed acyclic graph where the first layer holds its inputs, the second layer holds its processing units (the neurons, which are activated through mathematical functions) and the third layer holds its calculated outputs. In learning process, the structure links' weights are repeatedly adjusted so it develops a good prediction power; when this process is over, this structure is responsible for generating right outputs.

The ANN proposed here has a (2, 3) ANN configuration (that is, two neurons in the first sub-processing layer and three neurons in the last sub-processing layer) as pictured in Fig. 8. It requires three  $I - V$  points as inputs to predict the system's  $I_{mp}$  and uses resilient backpropagation with weight backtracking [14], softplus [15] as the neurons' activation function and sum of squared errors as the ANN's cost function. The three operating points are chosen so they fit different curves (Fig. 9) and the ANN has an accuracy of 99.51%. Although [16] shows that a higher number of operating points as inputs elevate the ANN precision, it deals with nonconvex characteristic curves. When using DCR, the sampling process can be reduced while keeping significant accuracy, as shown through the ANN proposed here. Fig. 10 shows the mapping of the actual and this configuration's estimated  $I_{mp}$  values.

The ANN was generated through R's `neuralnet` package [17]. The training and test sets were composed of 70% and 30% of a 290 different 3 : 2 ladder DCR string simulated curves base, respectively.

The proposed solution can be further explored by adding the PV's temperature  $T$  as an input to the ANN. This parameter shows good results in ANNs used for MPPT in standard PV structures [18], [19].

#### V. CONCLUSION

This work explores an integrated solution of DCR together with an ANN based MPP prediction method.

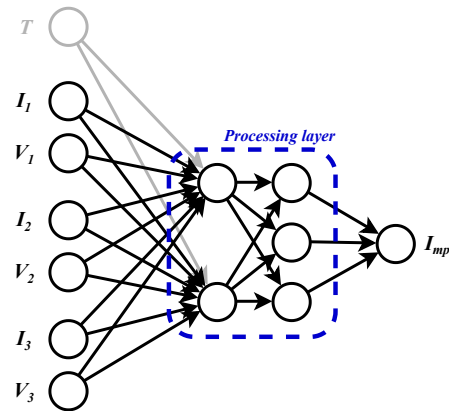


Fig. 8. Proposed ANN structure. The PV's temperature  $T$  is an additional and possible input.

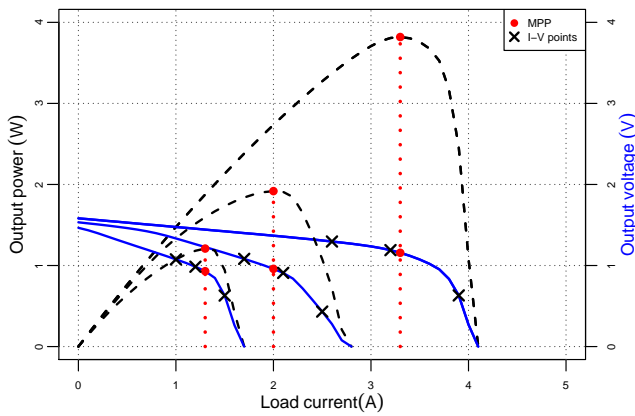


Fig. 9. Proposed ANN's  $I - V$  points sampling applied to the 3 : 2 ladder DCR string under different shading conditions.

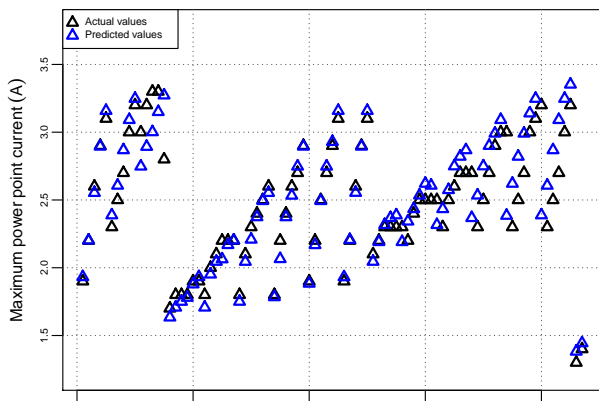


Fig. 10. Proposed ANN prediction power.

The simulations of a 3 : 2 ladder string using DCR shows that the strategy can raise the MPP of mismatched PVs by near 60% without affecting their default convex characteristics.

The MPP prediction method proposed for this structure is ANN based and can predict the 3 : 2 ladder DCR string's  $I_{mp}$  using only three of its operating points as inputs. This reduces the sampling time of the MPPT process, which can show a better performance since it adjusts its system's operating point in real time. The solution has an accuracy of 99.51% and a (2, 3) configuration. This ANN can be implemented in Verilog/VHDL for on-chip integration together with the switches and drivers of the DCR strategy, being suitable for PV applications such as IoT.

DCR can be further explored by studying different ladder configurations and different MPPT methods that could better fit it.

#### ACKNOWLEDGMENT

The authors would like to thank the Group of Integrated Circuits and Systems (GICS) of the Federal University of Paraná for providing the Cadence simulation environment used in the development of this work.

#### REFERENCES

- [1] H. Islam et al., "Performance Evaluation of Maximum Power Point Tracking Approaches and Photovoltaic Systems," *Energies*, vol. 11, no. 2, p. 365, Feb. 2018, doi: 10.3390/en11020365.
- [2] J. Cubas, S. Pindado, Á. Sanz-Andrés, "Accurate Simulation of MPPT Methods Performance When Applied to Commercial Photovoltaic Panels," *The Scientific World J.*, vol. 2015, pp. 1–16, 2015, doi: 10.1155/2015/914212.
- [3] S. K. Dash, S. Nema, R. K. Nema, D. Verma, "A comprehensive assessment of maximum power point tracking techniques under uniform and non-uniform irradiance and its impact on photovoltaic systems: A review," *J. Renewable Sustain. Energy*, vol. 7, no. 6, pp. 89–98, Nov. 2015, doi: 10.1063/1.4936572.
- [4] J. C. Teo, R. H. G. Tan, V. H. Mok, V. K. Ramachandaramurth and C. Tan, "Impact of Partial Shading on the P-V Characteristics and the Maximum Power of a Photovoltaic String," *Energies*, vol. 11, no. 7, p. 1860, July 2018, doi: 10.3390/en11071860.
- [5] A. Rao, R. Pillai, M. Mani and P. Ramamurthy, "Influence of Dust Deposition on Photovoltaic Panel Performance," *Energy Procedia*, vol. 54, pp. 690–700, 2014. doi: 10.1016/j.egypro.2014.07.310.
- [6] J. C. Teo, R. H. G. Tan, V. H. Mok, V. K. Ramachandaramurth and C. Tan, "Effects of bypass diode configurations to the maximum power of photovoltaic module," *Int. J. of Smart Grid and Clean Energy*, vol. 6, no. 4, pp. 225–232, Oct. 2017, doi: 10.12720/sgece.6.4.225-232.
- [7] H. Zheng and S. Li. Young, "Design of Bypass Diodes in Improving Energy Extraction of Solar PV Systems under Uneven Shading Conditions," in *Proc. T&D Conf. and Expo.*, 2014, pp.1–5, doi: 10.1109/TDC.2014.6863390.
- [8] A. H. Chang, A. T. Avestruz and S. B. Leeb "Capacitor-Less Photovoltaic Cell-Level Power Balancing Using Diffusion Charge Redistribution," *IEEE Trans. Power Electronics*, vol. 30, no. 2, pp. 537–546, Feb. 2015, doi: 10.1109/TPEL.2014.2340403.
- [9] M. R. Elhebeary, M. A. A. Ibrahim, M. M. Aboudina and A. N. Mohieldin, "Dual-Source Self-Start High-Efficiency Micro-Scale Smart Energy Harvesting System for IoT Applications," *IEEE Trans. Industrial Electronics*, vol. 65, no. 1, pp. 342–351, Jan. 2018, doi: 10.1109/TIE.2017.2714119.
- [10] A. R. Reisi, M. H. Moradi and S. Jamsab, "Classification and comparison of maximum power point tracking techniques for photovoltaic system: A review," *Renewable and Sustain. Energy Reviews*, vol. 19, pp. 433–443, Mar 2013, doi: 10.1016/j.rser.2012.11.052.
- [11] A. N. Celik and N. Acikgoz, "Modelling and experimental verification of the operating current of mono-crystalline photovoltaic modules using four- and five-parameter models," *Appl. Energy*, vol. 84, no. 1, pp. 1–15, Jan. 2007, doi: 10.1016/j.apenergy.2006.04.007.
- [12] M. D. Seeman, "A design methodology for switched-capacitor DC–DC converters," Ph.D. dissertation, Dept. EECS, Univ. California, Berkeley, USA, May 2009.
- [13] S. O. Haykin, *Neural Networks and Learning Machines*, 3rd ed. Ontario, Canada: Prentice-Hall, 2009.
- [14] M. Riedmiller, "Rprop - Description and Implementation Details," Univ. Karlsruhe, Baden-Württemberg, Germany, W-76128, Jan. 1994.
- [15] C. Dugas, Y. Bengio, F. Bélisle, C. Nadeau, and R. Garcia, "Incorporating Second-Order Functional Knowledge for Better Option Pricing," *Advances in Neural Inf. Process. Systems*, vol. 13, pp. 472–478, Feb. 2001.
- [16] S. A. Rizzo and G. Scelba, "ANN based MPPT method for rapidly variable shading conditions," *Appl. Energy*, vol. 145, pp. 124–132, May 2015. doi: 10.1016/j.apenergy.2015.01.077.
- [17] S. Fritsch, F. Guenther and M. N. Wright. *neuralnet: Training of Neural Networks*. (2019). Accessed on: June 02, 2019. [Online]. Available: <https://cran.r-project.org/web/packages/neuralnet/neuralnet.pdf>.
- [18] K. Arthishri, R. Balasubramanian, P. Kathirvelu, S. P. Simon and R. Amirtharajan, "Maximum Power Point Tracking of Photovoltaic Generation System using Artificial Neural Network with Improved Tracking Factor," *J. of Appl. Sciences*, vol. 14, no. 16, pp. 1858–1864, 2014, doi: 10.3923/jas.2014.1858.1864.
- [19] L. M. Elobaid, A. K. Abdelsalam and E. E. Zakzouk, "Artificial Neural Network Based Maximum Power Point Tracking Technique for PV Systems," in *Proc. 38th Annu. Conf. IEEE Ind. Electronics Soc.*, December 2012, pp. 937–942, doi: 10.1109/IECON.2012.6389165.